THE ASTROPHYSICAL JOURNAL, 283:580–597, 1984 August 15

A SEARCH FOR DISTANT HALO RR LYRAE STARS

A. SAHA
Palomar Observatory, California Institute of Technology
Received 1983 December 21; accepted 1984 February 29

ABSTRACT

The 48 inch (1.2 m) Schmidt telescope on Palomar mountain has been used to search for faint RR Lyrae stars in selected regions of the galactic halo. Results are presented here for three fields centered at $l = 180°$, $b = 24°$; $l = 180°$, $b = 30°$; and $l = 110°$, $b = -30°$. The faint limit for finding RR Lyrae stars is 19.5 mag in mean *B*, and the faintest RR Lyrae stars that were found are at galactocentric distances of over 40 kpc. The majority of the stars are 20–30 kpc from the galactic center and typically around 18 mag in *B*. Apart from a very few globular clusters, these are the most distant known probes of the outer halo.

Photoelectric photometry has been used to obtain accurate light curves and ephemerides for all the survey RR Lyrae stars. These data are necessary before spectroscopy of these objects can be performed and interpreted correctly.

The survey has also identified a large number of faint eclipsing stars, mainly of the W UMa type. It is very likely that many of these are halo objects, and spectroscopic studies to determine their abundances and kinematical affiliation are recommended.

Subject headings: galaxies: Milky Way — galaxies: stellar content — galaxies: structure — stars: RR Lyrae

I. INTRODUCTION

It is well known that RR Lyrae stars are very valuable probes of the galactic halo. They are readily detectable on the basis of their characteristic light variation and are perhaps the best calibrated distance indicators. They constitute a kinematically unbiased sample (provided that stars with different abundances within the halo do not belong to different kinematic groups), and it is possible to find large numbers of them out to very large distances. The kinematics of the brighter field RR Lyrae stars, many of which are members of the halo, have been studied by Woolley (1978). The Lick Astrograph survey (Kinman *et al.* 1982 and references therein) has identified faint RR Lyrae stars out to 25 kpc from the galactic center, and Butler *et al.* (1982 and references therein) have investigated the abundance distribution in the halo gleaned from the spectroscopy of these stars. It is only recently that it has become possible to measure radial velocities of these faint RR Lyrae stars with sufficient accuracy to study halo kinematics.

This work pushes the search for RR Lyrae stars to yet fainter magnitudes, and hence to regions even farther out in the halo. Use of the Palomar 48 inch (1.2 m) Schmidt telescope and of newer, more suitable photographic emulsions has made it possible to find RR Lyrae stars to as faint as 19.5 mag in mean *B*, or out to 50 kpc from the galactic center, which is twice the distance reached by the Lick Astrograph survey. Using these stars, we are able to probe the extent, abundance content, and kinematical properties (and hence the mass distribution) of the distant halo.

This paper describes the discovery and photometry of the RR Lyrae stars. Light curves and ephemerides of these objects are presented. Spectroscopic and spectrophotometric measurements have been made and analyzed, and the results from them and their bearing on the space distribution, chemical abundance gradients, and kinematics of the halo will be the subject of another paper.

II. OBSERVATIONS

The plates for the survey were taken with the 48 inch (1.2 m) Schmidt telescope on Palomar mountain. Kodak IIIa-J emulsion 14 × 14 inch (36 × 36 cm) plates were used with a Kodak Wratten 4 filter. This combination allows a bandpass from 4600 Å to 5400 Å, and corresponds to the "*g*" filter in the Thuan and Gunn (1976) photometric system. Since this passband is in a region where there are no significant night sky emission lines, and since the emulsion has fine grain and high contrast, very deep plates are possible with this combination. Each plate covers an area of approximately 6°.6 × 6°.6. There is no vignetting within the central 12 inch (30 cm) diameter circle of the plate.

The plates were sensitized by baking them in forming gas at 65°C for 2 to 2.5 hours (depending on the batch). After exposure they were processed for 5 minutes in Kodak D-19 developer at 19°C. The time required for a sky-limited exposure is then about 2.5 hours, and when the seeing is 3″ or better, stellar images to 22 mag can be detected.

For the purposes of the survey, a faint limit of 20 mag was considered adequate. Four separate 30 minute exposures of each field were taken on the same plate, and the telescope was moved about 12″ between exposures. In this way, for every star in the field, there are four identical images on the plate arranged in a line. As long as the average spacing between objects in the field is not smaller than 0′.5, there is no difficulty in identifying separate sets of four images that all belong to the same star. The time between successive exposures was typically 1.5–2 hours. It is possible to remove the plate-holder from the telescope and reinsert it without appreciable change in the positioning of the plate, provided the plate itself is not removed from the plate-holder. Thus while waiting for the 1.5–2 hours to elapse between successive exposures on the same plate, it was possible to take out the plate-holder, and expose plates of other fields by using different plate-holders for each plate. It was possible, through this cycle, to obtain four-image plates for three different fields on the same night, thus making maximum use of the telescope.

This multiple-image technique emulates the methods described by Kinman (1972). Its advantage is in reducing the labor involved in manually comparing different exposures, as well as in cutting down the cost of plate material used by a factor of 4 (in this case). When a plate is scanned, the four images of each star are compared to check for variability. In scanning one plate, six pairs (four images taken two at a time) of images are compared, as opposed to one pair when two single image plates are blinked. Although the blink process is more efficient and easier to perform manually, this factor of 6 gain appreciably reduces the total labor performed.

Table 1 is the list of fields for which plates were taken.

III. DETECTION OF VARIABLE STARS

The plates described above were scanned by eye. The faint limit on the plates is approximately 20 mag. Due to the high contrast of IIIa-J emulsions, the images are saturated at about 16.5 mag. Small differences in magnitude are more easily recognized when the images are unsaturated. For brighter objects, where the images are saturated, brightness is judged by the size of the image rather than by the density, and so the sensitivity to a change in brightness is poorer. A change of 0.3 mag can be readily detected (by visual inspection) for objects between 16.5 mag and 19.5 mag, but for objects brighter than 16.5 mag, the change must be much larger before it can be detected with confidence. The discussions regarding completeness of the survey will be restricted to the magnitude interval 16.5–19.5 mag. Some variable objects were found at brighter magnitudes, and if so they were noted. At these bright magnitudes, only objects with appreciably higher amplitudes of light variation could be found, and the selection effects are very complicated.

Several plates of each field were scanned. Work has been completed for fields FII, FIII, and FIV (see Table 1). From the way the plates were taken and images compared, only objects whose brightnesses change over durations of a few hours would be detected. Thus only objects with periods of a day or smaller were expected. In each of the above fields about 30 variable stars were found, but it was not immediately known which were RR Lyrae stars, and which were other types of short-period variables. To be able to make this distinction, it is necessary to obtain light curves for the objects.

An obvious approach is to photoelectrically measure and define standard stars in each field, and then use these to calibrate iris photometer measurements made on the plate and thus measure magnitudes of the variable stars. However, severe difficulties were encountered in attempting such measurements. The Schmidt telescope makes images at f/2.5. Even slight errors in positioning the plates (due to defects in the plate-holder, inaccuracy in focusing, etc.) means that images in one part of the plate are focused slightly differently from those in another part of the same plate. Since the resulting image characteristics are quite different in different parts of the field, and since the plate response is of course nonlinear, the iris-photometry calibrations change from one section of the plate to another. Ironically, this effect is more pronounced on finer grain emulsions which resolve the change in image contours than on coarser grain emulsions that do not resolve this effect. The nonuniformity of the IIIa-J emulsion over the entire plate surface is another likely contributor to the calibration errors. Within the unvignetted region of the plate, only a region with a 2 inch (5 cm) radius can be calibrated, and a different set of standards is required for each such section of the plate.

Since the aim was to separate the RR Lyrae stars from the rest, it was realized that the periods and light-curve asymmetry can be obtained without reference to a bona fide magnitude scale. About 10 stars around each variable star were chosen so that their magnitudes span the range of variability of the object under study, and the brightness of the variable could be placed relative to these surrounding stars. These arbitrary "magnitude" measurements could then be used to derive periods using the technique of Lafler and Kinman (1965).

The pseudo–light curves so obtained do contain the period and asymmetry information. Light curves that showed asymmetry were immediately spotted as pulsating variables (all type *ab* RR Lyrae stars have asymmetric light curves), and were picked out for further study with photoelectric techniques. Those that showed two unequal "dips" and symmetric light curves were identified as eclipsing variables. It is not possible to distinguish between *c*-type RR Lyrae stars and eclipsing stars which have only one discernible eclipse (or two equal eclipses), except when the periods are too short or too long for them to be RR Lyrae stars. These ambiguous cases were also selected for further study.

IV. COMPLETENESS OF THE SAMPLE

In a survey of this kind, it is very important to pay close attention to selection effects and incompleteness. In the present case there are mainly three factors that produce incompleteness in the sample. They are discussed one by one.

First, there are limitations due to the dynamic range of the detector. As mentioned before, a change of 0.3 mag can be detected if the object lies in the magnitude interval 16.5–19.5 during at least one of the observed phases. This discussion will be restricted to objects that have amplitudes >0.4 mag and lie, during some part of their light cycle, in the above stated magnitude interval. The amplitude criterion is sufficient to include RR Lyrae stars of all Bailey types.

The second factor will be called "detectability." The procedure followed in scanning the plates, as described in § III, effectively checks for objects that have changed in brightness over a few hours. Objects that have periods less than 90 minutes fall out of the scope of this discussion. An object which does not change by at least 0.3 mag during any 6 hour interval (or less) is also outside the domain of this discussion. Thus Cepheids and other relatively longer period variables are excluded, but RR Lyrae stars and many short-period binary stars fall within the purview of the following analysis. Although RR Lyrae stars have periods of up to 0.8 days, there is always a

TABLE 1

POSITIONS OF FIELD CENTERS

Field Name	Guide Star Coordinates (1950) (Plate Center)		Galactic Coordinates	
	R.A.	Decl.	l	b
FI	$6^h57^m24\overset{s}{.}1$	37°11′59″	179°.7	17°.7
FII	7 28 32.2	39 00 11	180.0	24.1
FII	7 58 24.9	40 17 06	180.2	30.0
FIV	23 56 15.9	32 06 13	110.2	−29.2
FV	9 48 50.7	−13 29 32	250.3	30.2
FVI	3 56 55.9	10 11 23	180.1	−31.0
FVII	8 31 43.7	41 54 34	179.5	36.4

section of their light curve, particularly during the rapid rise to maximum light, which satisfies the last criterion. Similarly, objects with eclipses that are at least 0.3 mag deep and have durations shorter than 12 hours are included in this analysis. Without any loss of generality, we can, for the present discussion, assign the phase ϕ at which this criterion of rapid change of intensity is satisfied, to be equal to zero. If the first and last images on any given plate were taken at times t and t' respectively, then an object that passed through $\phi = 0$ between t and t' is expected to be "detectable" on that plate. There are periodicities associated with the plate observations: chiefly the night-to-night period of 1 day and the lunation period of 1 month. By working according to a predetermined schedule, some of the effects of these can be minimized. However, even the best laid plans are subject to the interference of weather conditions.

Finally, there are the human errors associated with the plate scanning itself. These are the hardest to describe objectively, but an *a posteriori* analysis is given below. From this analysis, it is possible to derive the "efficiency" of the scanning. The efficiency index η measures the fraction of objects that were detected on any given plate, as opposed to the number of "detectable" objects on that plate. It is estimated by cross-comparing the results of scanning several plates of the same field and the derivation is as follows.

Let N_i be the number of detectable objects on the ith plate of any field. Let n_i be the number of objects actually detected on that plate. Let β_{ij} be the scanning efficiency that will be derived for plate i by comparing against plate j of the same field. We then have:

$$n_i = \beta_{ij} N_i \,. \tag{1}$$

Let n_{ij} denote the number of objects detected on both plates i and j, and let $n_{i\bar{j}}$ denote the number of objects "detectable" on both plates, but found only on plate i and not on plate j. Thus:

$$n_{ij} = \beta_{ij} \beta_{ji} N_{ij} \,,$$

where N_{ij} is the number of objects that are detectable on both plates. Also,

$$n_{i\bar{j}} = \beta_{ij}(1 - \beta_{ji}) N_{ij} \tag{2a}$$

and

$$n_{j\bar{i}} = \beta_{ji}(1 - \beta_{ij}) N_{ij} \,. \tag{2b}$$

It follows that

$$\beta_{ij} = \frac{n_{ij}}{(n_{j\bar{i}} + n_{ij})} \,. \tag{3}$$

The various plates of each field were compared after scanning to find the quantities n_{ij} and $n_{i\bar{j}}$ for all i and j, and the β_{ij}'s were calculated according to equation (3). The final adopted value η_i for the efficiency with which the ith plate was scanned was taken to be the weighted (by n_{ij}) average (over j) of β_{ij}:

$$\eta_i = \frac{\sum_j n_{ij} \beta_{ij}}{\sum_j n_{ij}} \,, \tag{4}$$

where $i \neq j$. Table 2 shows the values of η_i's that were found for the plates of the three different fields.

It was stated earlier than an object is considered to be "detectable" if it passes through phase $\phi = 0$ during the time spanned by the four exposures on that plate. Consider an object with period P which has $\phi = \phi_0$ at some fiducial time (before any plates were taken) $t = 0$. Consider a plate on which the first exposure was at time t_1 and the last exposure was at time t_2. According to the stipulated criterion, the object is detectable on the plate if there exists some integer K, and some t such that for $t_1 < t < t_2$,

$$t = (K - \phi_0)P \,. \tag{5}$$

By testing if the criterion in equation (5) is satisfied, it can be determined if an object with period P and initial phase ϕ_0 is detectable on a given plate. For a given period P and initial phase ϕ_0, define

$$\rho_i = \begin{cases} \eta_i & \text{if object is detectable} \\ 0.0 & \text{if not detectable} \,. \end{cases} \tag{6}$$

The probability that this object is not detected on any of the N plates is then given by

$$\bar{p}(P, \phi_0) = \prod_{i=1}^{N} (1 - \rho_i) \,, \tag{7}$$

where $\bar{p}(P, \phi_0)$ is the probability of *not* finding an object with period P and initial phase ϕ_0. By assuming that all values of ϕ_0 (between 0 and 1) are equally likely, the probability $p(P)$ with

TABLE 2

PLATES SCANNED

Field	Plate No.	Julian Date of First Exposure	Julian Date of Last Exposure	Scanning Efficiency η
FII	1	2,444,258.697	2,444,258.870	0.71
	2	2,444,260.647	2,444,260.801	0.71
	3	2,444,261.782	2,444,261.887	0.77
	4	2,444,582.808	2,444,582.961	0.81
	5	2,444,583.911	2,444,583.935	0.81
	6	2,444,639.652	2,444,639.934	0.72
	7	2,444,992.646	2,444,992.949	0.74
FIII	1	2,444,639.681	2,444,639.959	0.84
	2	2,444,640.676	2,444,640.966	0.84
	3	2,444,947.830	2,444,948.035	0.77
FIV	1	2,444,582.613	2,444,582.779	0.70
	2	2,444,910.629	2,444,910.849	0.86
	3	2,445,200.752	2,445,200.979	0.65
	4	2,445,199.796	2,445,199.980	0.79

which an object with period P *is detected* on the N plate can be calculated as follows:

$$p(P) = \int_0^1 [1 - \bar{p}(P, \phi_0)] d\phi_0 \, . \quad (8)$$

The calculations pertaining to equations (5) through (8) were performed numerically.

Figure 1*a* is a plot of $p(P)$ versus P for a plate that spans 6 hours on one night, and where η has been taken to be 0.8. Figure 1*b* shows the improved probability of discovery when two such plates taken on adjacent nights are considered. Figure 1*c* is a plot of the same where plates from six consecutive nights are taken together. Note how the selection effects due to periodicity in the period range of the RR Lyrae stars is reduced as the number of nights is increased. Note also the difficulty of detecting variables with periods at or around one-third day, one-half day, two-thirds day, etc. Figure 2 illustrates the discovery probabilities for the plates that were actually examined. Results for each of the three fields studied are shown. These plots show more rapid variation with P because the plates were not taken on consecutive nights (because weather or seeing conditions would not permit). The larger the number of days that elapse between successive observations, the more "grassy" the plot appears.

This method of *a posteriori* analysis is a very realistic representation of selection effects arising from periodicity in the data.

V. COORDINATE MEASUREMENT

To ascertain the coordinates of the variables that were detected, X and Y positions of the objects were found using the comparator ("X-Y machine") at the offices of the Mount Wilson and Las Campanas Observatories. Position standards were chosen from the SAO catalog. Existing computer software was used to perform the necessary calculations. Coordinates accurate to about 2″ were derived. The positions of all the stars for which photometric light curves have been obtained are listed in Table 3, and the corresponding finding charts are in Figure 3 (Plates 14, 15 and 16). Some of the stars in FII and FIII were originally discovered by Kinman *et al.* (1982). In Table 3, their nomenclature for these stars are shown within parentheses.

VI. PHOTOMETRY AND EPHEMERIDES OF RR LYRAE CANDIDATES

Photoelectric photometry of the variable stars that are listed in Table 3 was done with the SIT Vidicon direct camera at the Cassegrain focus of the 60 inch (1.5 m) telescope on Palomar

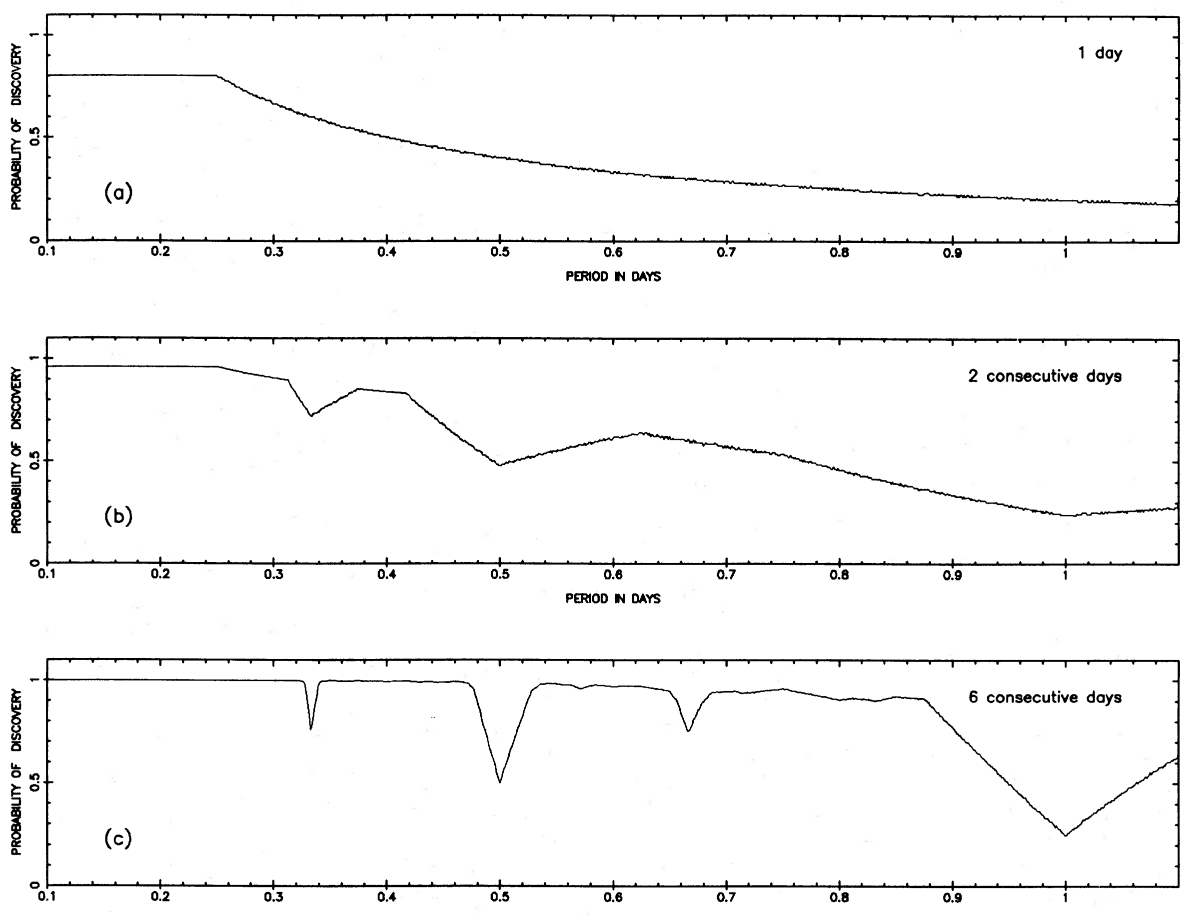

FIG. 1.—The diagrams show the probability of discovery (assuming a scanning efficiency of 0.8 for each plate) as a function of period. Fig. 1*a* shows the result of scanning a single plate where the four exposures span a total time interval of 6 hours on one night. Fig. 1*b* shows the result when two such plates from two consecutive nights (i.e., 24 hours apart) are scanned, and Fig. 1*c* shows the result of scanning six such plates taken on six consecutive nights.

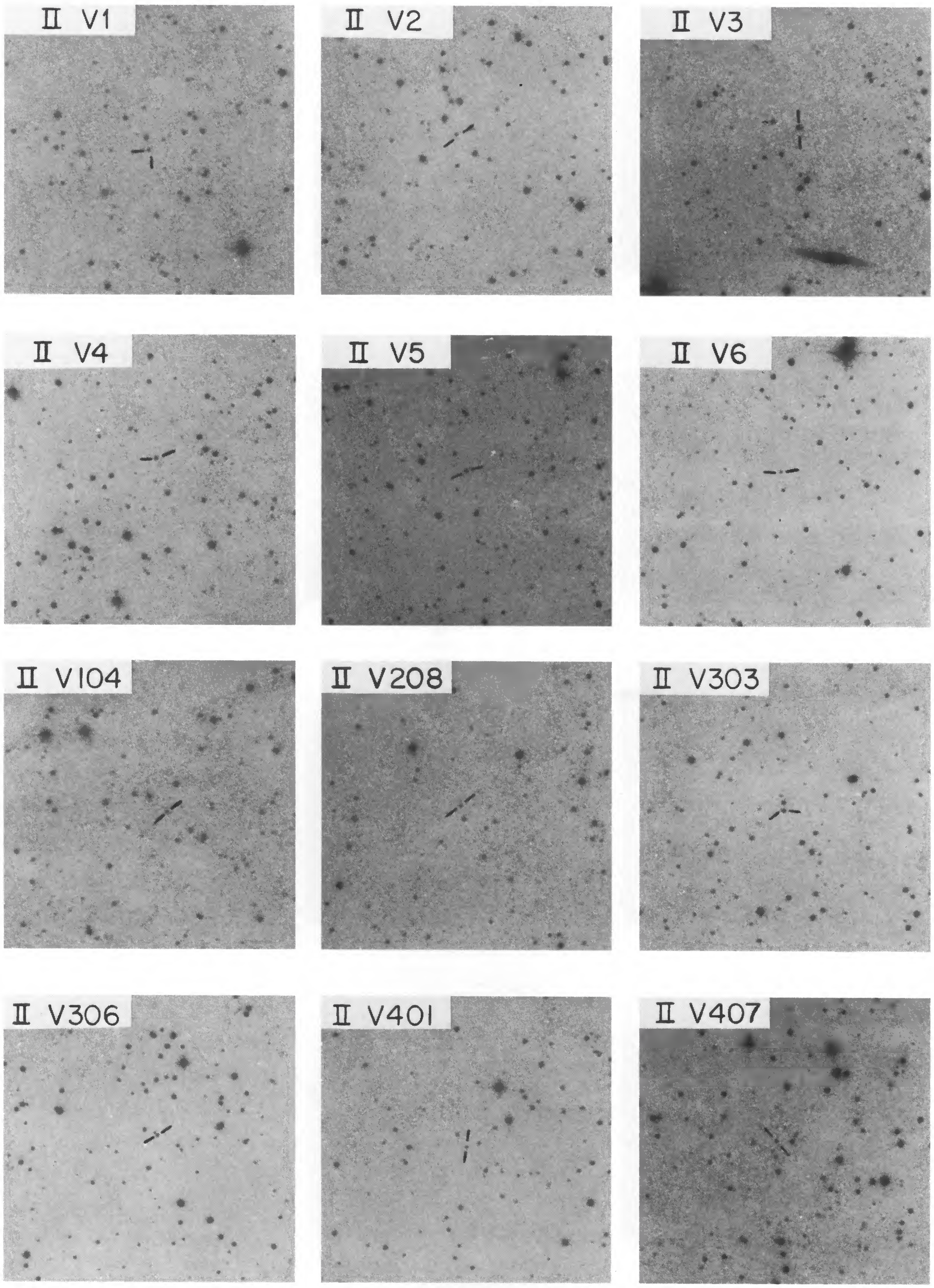

FIG. 3.—Finding charts for the variable stars listed in Table 3. North is up, and East is to the left. The scale is approximately 13″ per mm.

SAHA (*see* page 583)

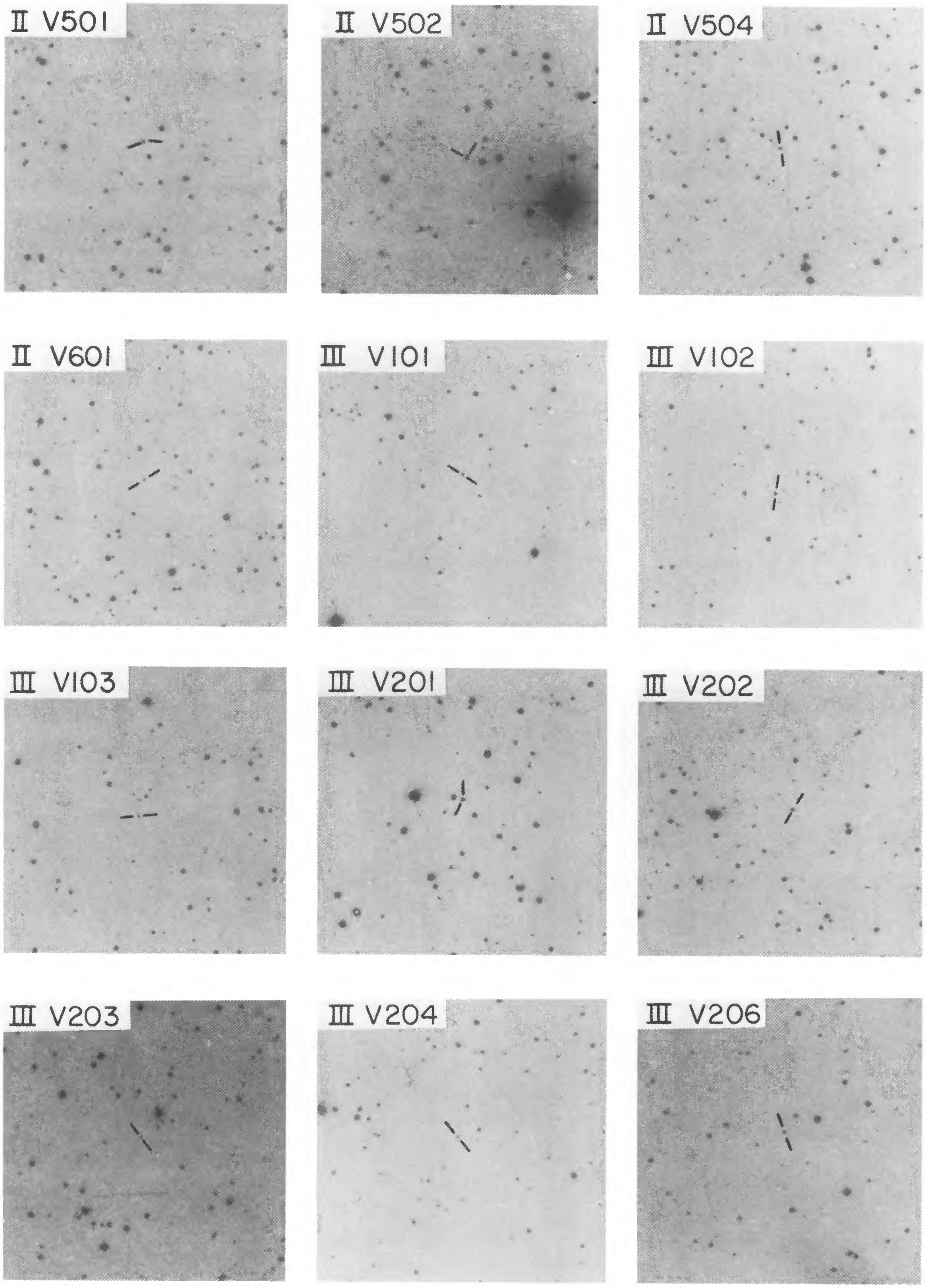

FIG. 3.—*Continued*

SAHA (*see* page 583)

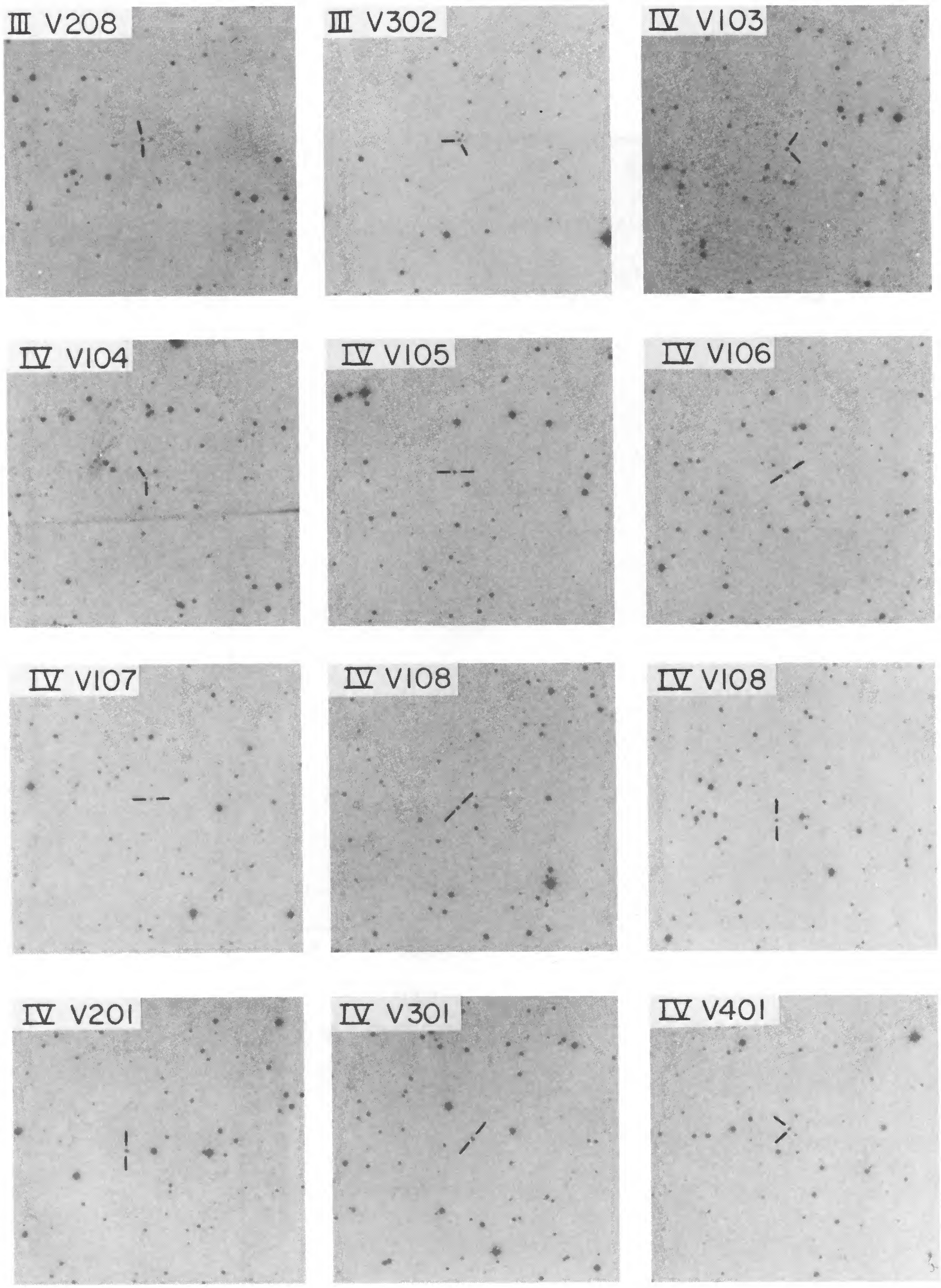

FIG. 3.—*Continued*

SAHA (*see* page 583)

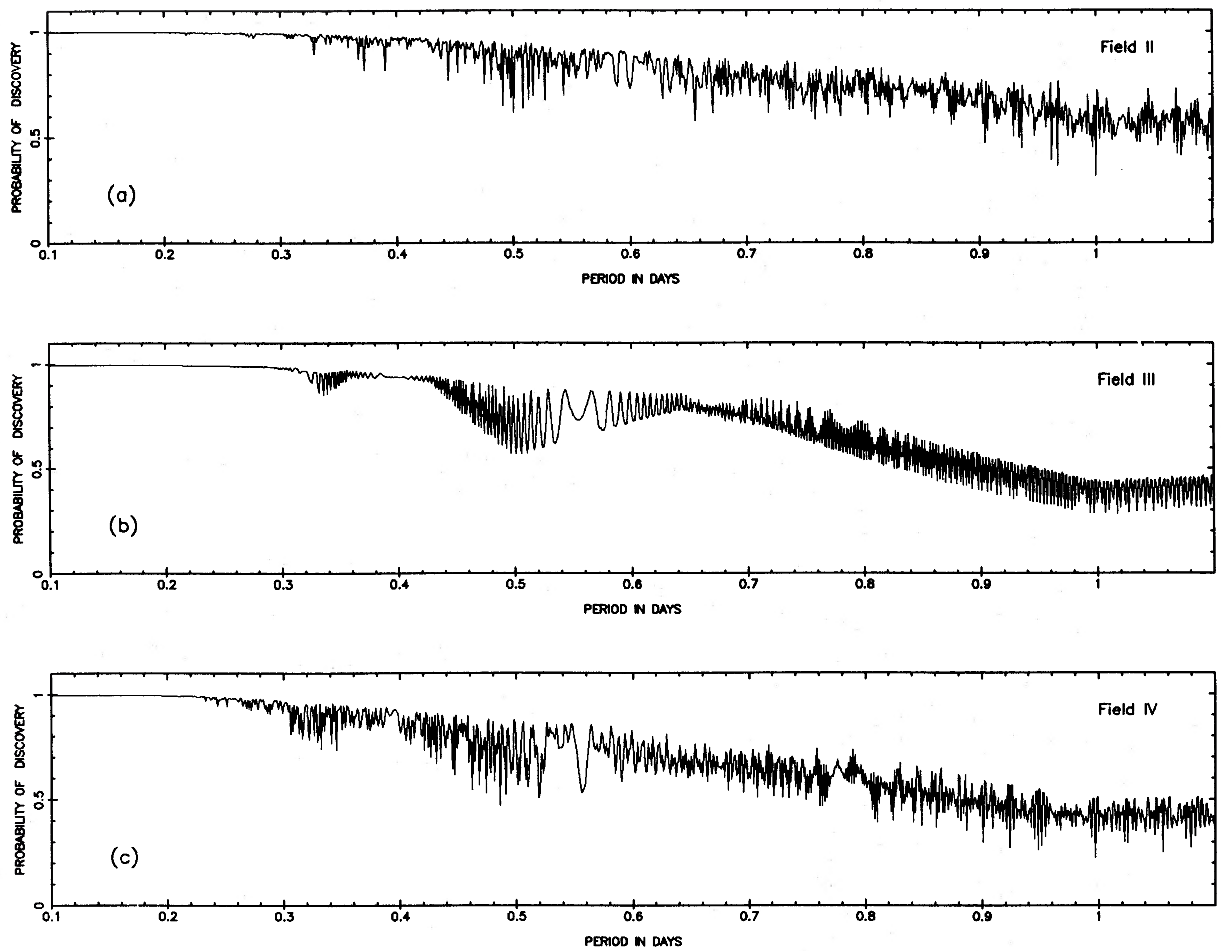

FIG. 2.—These plots show the probability of discovery as a function of period in the three fields that were scanned. The actual times of exposure have been used to estimate the probabilities according to the arguments given in § III.

mountain. The purpose was to obtain reliable light curves in B for the RR Lyrae stars. The light curves so obtained are then compatible with the available literature on other RR Lyrae stars, both in the field and in globular clusters. Also, light curves obtained from photoelectric photometry help to discriminate between W UMa stars and the c-type RR Lyrae stars, and all the doubtful cases could be tested in this way.

There are distinct advantages in using an area photometer over a one or two channel photometer when measuring faint stars. At 18th and 19th mag, sky subtraction must be done very accurately. If the object being measured has magnitude m, then the sky patch that is used for sky subtraction must not be contaminated by an object brighter than $m + 5$ if systematic errors are to be kept to within a few percent. This means that the observer must be able to see several magnitudes fainter than the object under study. Since crowding effects get progressively worse as one goes fainter, this problem merits greater attention at the faint magnitudes involved here. By the time an SIT camera picture is well enough exposed to get good photon statistics on the object, it is possible to detect objects several magnitudes fainter, so that they can be avoided when choosing a suitable sky patch. Second, with an area photometer it is possible to do "differential photometry," i.e., a star adjacent to the object of interest, which lies in the field of the camera (in this case a $3' \times 3'$ field), can be used as a comparison standard. The error in a single measurement of an object, when calibrated against a standard star in another part of the sky, is much larger than the error incurred in comparing two objects adjacent to each other which are measured simultaneously. Of course, the comparison object in the field has to be calibrated against a suitable standard to make the zero point adjustment, but here the average of several observations is taken, which decreases the random errors. For constructing light curves, where each individual observation is to be used as a data point, the scatter is considerably reduced by using such a technique. Further, at the time that the project was begun, there was no available TV viewer, so that acquiring the faint objects on an aperture of a conventional photometer was impossible, to say nothing of choosing an appropriate sky patch for sky subtraction.

The SIT tube of the camera has an S20 photocathode. However, the construction of the SIT camera precludes the use of liquid $CuSO_4$ cells, so the standard B filter described by Sandage and Smith (1963) could not be used. A modified B filter, using Schott BG38 as the red leak eliminating element, was specially constructed. The thicknesses of the other elements, namely Schott BG12 and GG385 were also altered to compensate for the response changes that the BG38 introduces within the passband. The filter employed has 1 mm BG12, 2 mm GG385, and 3 mm BG38.

Whenever possible, observations were made so that the comparison object for differential photometry was in the same

TABLE 3

COORDINATES OF VARIABLE STARS

Object	α	δ
Field II (Epoch 1950.0)		
II V1	$07^h41^m53^s.1$	+40°38′05″
II V3 (RR 40)	07 37 22.1	+39 25 51
II V5	07 13 23.3	+38 38 56
II V104 (RR 34)	07 28 28.5	+39 14 11
II V303	07 28 06.5	+40 11 34
II V401 (RR 45)	07 42 16.0	+40 29 51
II V501 (RR 43)	07 41 23.7	+40 19 59
II V504	07 22 45.5	+40 58 53
II V2	07 31 04.4	+40 43 31
II V4	07 23 44.7	+38 54 15
II V6	07 26 48.0	+38 28 11
II V208 (RR 38)	07 32 14.4	+39 22 07
II V306	07 23 41.0	+36 44 51
II V407	07 14 44.2	+40 36 41
II V502	07 37 06.0	+41 18 36
II V601	07 22 33.1	+38 18 59
Field III (Epoch 1950.0)		
III V101	08 00 13.1	+42 39 15
III V103	07 56 25.0	+39 24 44
III V202	07 50 41.0	+42 56 59
III V204 (RR 50)	07 51 20.8	+39 02 15
III V208	07 57 06.2	+40 47 42
III V102	07 53 55.7	+43 20 34
III V201 (RR 46)	07 47 02.1	+37 49 37
III V203	07 46 08.4	+41 50 32
III V206	08 06 11.4	+42 42 23
III V302	08 01 09.7	+42 37 34
Field IV (Epoch 1950.0)		
IV V101	00 05 58.4	+29 08 58
IV V104	23 53 12.2	+28 53 11
IV V106	23 44 25.7	+29 34 23
IV V108	00 04 23.5	+31 45 26
IV V201	00 04 21.3	+31 11 17
IV V401	00 03 33.0	+29 02 12
IV V103	23 59 41.3	+29 47 55
IV V105	23 42 06.2	+29 53 31
IV V107	23 54 13.6	+31 23 40
IV V122	00 08 04.0	+33 50 16
IV V301	00 08 57.3	+30 34 42

picture as the object. In the few cases where this was not possible, the closest feasible local comparison object was exposed either immediately before or after the object. The photometric standards of Thuan and Gunn (1976) were observed on the nights when photometric conditions were pristine, so that the local comparison standards (LCS) could be calibrated.

The pictures obtained in this way were reduced (using a program written by W. L. Sebok) to obtain instrumental magnitudes for the objects, the LCS and the photometric standards. Sky and object "apertures" were simulated in software, and the device response was assumed to be linear. Details regarding the reduction prescription that account for the peculiarities of this particular instrument are described in Saha (1983).

The magnitudes of the LCS were calibrated against the Thuan and Gunn (1976) standards. The atmospheric extinction was derived for each night using observations of the standard stars at different air masses. Color corrections were not applied, since an adequate number of observations in other colors was not possible. The error introduced by ignoring color corrections does not exceed 0.02 mag for the air masses at which observations were made. Once the brightness of the LCS were established, they were used to convert the magnitude differences between object and LCS to actual magnitudes for the object.

There remains the question of whether the device is truly linear as assumed in the reductions. This is particularly important since 9th and 10th mag standards were used to calibrate magnitudes as faint as 20. Some of the stars in and around the globular cluster M3, whose *UBV* magnitudes are known from Sandage (1970), were observed with the SIT camera. These test stars were chosen to as faint as 19.4 mag in *B*. Repeated observations were made to keep the internal random errors in the measurement of each star to within 0.03 mag. The mean values thus obtained agree with those given by Sandage (1970) within a standard deviation error of 0.06 mag and show no systematic difference. No trend that could indicate nonlinearity was found.

The results of the photometric measurements are shown in Table 4. The first column shows the mean time of exposure in heliocentric Julian dates (HJD), and the second column shows the *B* magnitude measured in the way described above. The last entry for each object which shows HJD = 0.0, gives the magnitude of the pertinent local comparison standard.

The observations obtained in the above manner were used to obtain periods and epochs for the variable stars. The method of Lafler and Kinman (1965) was used. In some cases it is very difficult to distinguish between the true period and an alias period because of the periodicity in the observations themselves. In such cases, the dispute could often be resolved by looking at the possible periods obtained from the iris photometry of the plates (as described in § III). Despite all the care and precaution, it is not possible to guarantee that spurious periods do not occur. Only what appear to be the most likely values ("best" periods), are quoted in Table 5. The first column of Table 5 lists the object name, the second column gives the best determination of its period, and the third column is the accuracy to which the "best" period was determined. The fourth column gives the normalized value of the discriminant Θ (after Lafler and Kinman 1965):

$$\Theta = \frac{\sum_{i=1}^{N} (m_i - m_{i+1})^2}{\sum_{i=1}^{N} (m_i - \bar{m})^2} ,$$

where m_i is the magnitude for the ith observation arranged in increasing order of phase for a given trial period, and $\bar{m}$ is the mean of all the observed magnitudes. A lower value of Θ indicates a better determination of the light curve (smaller errors in photometry and/or better sampling in phase) and a greater likelihood that spurious periods have been eliminated. Although the exact interpretation of Θ as a light curve quality indicator is complicated and depends on the light curve shape itself, generally a value less than 0.30 is quite adequate. The fifth column gives the mean *B* magnitude $\langle B \rangle$. If the ith of N individual measurements of *B* for any object is denoted by B_i, $\langle B \rangle$ is given by:

$$\langle B \rangle = \log \sum_{i=1}^{N} 0.5(\phi_{i+1} - \phi_{i-1})10^{B_i} , \qquad (9)$$

where ϕ_i is the phase of the ith observation in order of increasing ϕ, and where it is implied that $\phi_0 = \phi_N$ and $\phi_{N+1} = \phi_1$. Thus $\langle B \rangle$ is a flux-averaged magnitude. The sixth column of Table 5 gives the epoch (heliocentric Julian date) of phase zero. The last column indicates the type of variable star that the

TABLE 4

SIT CAMERA DATA FOR LIGHT CURVES

HJD	B	HJD	B	HJD	B
II V1					
2444547.981	18.16	2444548.856	17.72	2444548.952	17.88
2444549.015	18.47	2444549.834	17.99	2444549.886	18.20
2444549.933	17.92	2444550.861	18.03	2444550.927	18.12
2444550.977	18.01	2444551.841	17.99	2444551.934	17.81
2444552.005	18.22	2444552.823	17.78	2444552.963	18.16
2444609.690	18.06	2444609.694	18.23	2444609.854	18.64
2444609.896	18.03	2444609.899	17.90	2444609.974	18.68
2444636.725	17.92	2444636.830	18.13	2444636.966	17.93
0.000	15.84(±.03)				
II V2					
2444547.983	18.25	2444548.861	17.95	2444548.954	18.33
2444549.020	17.92	2444549.841	18.43	2444549.888	18.33
2444549.936	18.07	2444550.865	18.12	2444550.930	18.62
2444550.980	18.11	2444551.848	18.78	2444551.937	18.14
2444552.008	18.21	2444552.833	17.83	2444552.904	18.67
2444552.967	17.99	2444609.694	18.53	2444609.769	18.32
2444609.858	18.54	2444609.902	18.14	2444609.906	18.05
2444609.977	18.92	2444609.981	18.88	2444636.728	18.76
2444636.732	18.98	2444636.834	18.36	2444636.839	18.37
2444636.970	18.32	0.000	16.11(±.02)		
II V3					
2444547.986	15.03	2444549.021	14.83	2444549.843	15.03
2444549.891	15.03	2444549.938	15.17	2444550.866	14.83
2444550.937	15.02	2444550.986	15.00	2444551.852	13.93
2444551.939	14.20	2444552.011	14.45	2444552.836	15.11
2444552.907	14.93	2444609.701	14.30	2444609.772	14.61
2444609.861	14.93	2444609.910	15.09	2444609.912	14.99
2444609.985	15.10	2444636.734	14.97	2444636.841	14.92
2444636.973	14.08			0.000	16.28(±.03)
II V4					
2444548.866	17.11	2444548.960	16.75	2444549.846	17.12
2444549.894	16.96	2444549.940	16.63	2444550.869	17.19
2444550.937	16.67	2444550.989	16.65	2444551.854	16.76
2444551.942	16.79	2444552.015	16.67	2444552.839	16.66
2444552.909	16.91	2444552.971	16.78	2444609.718	16.80
2444609.774	17.64	2444609.865	16.66	2444609.914	17.08
2444609.917	17.11	2444609.990	16.84	2444636.845	17.17
2444636.739	16.62	2444636.977	17.11	2444636.743	16.62
0.000	15.76(±.03)				

HJD	B	HJD	B.	HJD	B
II V5					
2444548.869	16.60	2444548.962	16.62	2444549.026	17.42
2444549.849	16.59	2444549.897	16.54	2444549.943	16.54
2444550.872	16.60	2444550.949	16.46	2444550.991	16.60
2444551.875	16.94	2444551.945	18.72	2444552.018	16.93
2444552.843	16.70	2444552.912	16.62	2444552.973	16.62
2444609.720	16.69	2444609.722	16.69	2444609.776	16.53
2444609.779	16.56	2444609.867	16.55	2444609.869	16.60
2444609.920	16.65	2444609.923	16.61	2444609.992	16.63
2444636.847	16.61	2444636.746	16.61	2444636.978	16.59
0.000	17.10(±.02)				
II V6					
2444548.870	18.29	2444636.745	18.19	2444636.847	17.79
2444636.979	17.82	2444609.720	18.31	2444609.724	18.16
2444609.777	18.42	2444609.867	17.24	2444609.921	17.57
2444609.927	17.58	2444609.991	17.89	2444552.850	18.15
2444552.915	18.36	2444552.973	17.29	2444551.880	17.32
2444551.945	17.59	2444552.018	17.86	2444550.873	17.84
2444550.950	18.17	2444550.995	18.16	2444549.852	18.22
2444549.897	18.30	2444549.943	18.29	2444548.963	18.29
2444549.027	17.37	2444994.824	18.26	2444994.830	18.34
2445322.757	17.49	2445322.761	17.44	2445355.912	18.40
2445355.920	18.34	2445355.929	18.06	2445355.934	17.78
2445355.939	17.70	2445355.947	17.61	2445355.952	17.48
2445355.962	17.36	2445355.967	17.34	2445355.971	17.17
2445355.975	17.21	2445355.980	17.30	0.000	18.20(±.04)
II V104					
2445323.779	17.72	2445323.784	17.74	2445323.866	16.99
2445323.946	16.83	2445324.016	17.27	2445324.764	17.84
2445324.944	17.59	2445324.991	16.47	2445325.019	16.51
2445327.878	17.03	2445354.865	16.79	2445355.761	17.71
2445355.803	17.60	2445355.857	17.66	2445355.892	17.49
2445349.780	17.79	2445349.697	17.71	0.000	16.88(±.02)
II V208					
2445323.791	16.91	2445323.872	17.15	2445323.950	17.34
2445324.021	17.34	2445324.767	16.67	2445324.949	17.03
2445324.992	17.19	2445325.024	17.28	2445327.887	17.41
2445328.053	17.06	2445349.679	16.55	2445349.688	16.50
2445349.704	16.58	2445349.783	16.94	2445354.872	17.27
2445354.876	17.34	2445355.779	16.54	2445355.797	16.60
2445355.799	16.61	2445355.862	16.79	2445355.896	17.13

TABLE 4—*Continued*

HJD	B	HJD	B	HJD	B
0.000	16.55(±.02)				
II V303					
2444548.885	16.26	2444548.973	15.86	2444549.042	15.77
2444549.868	15.63	2444549.907	15.66	2444549.957	16.27
2444550.884	16.32	2444550.962	15.66	2444551.004	16.39
2444551.888	15.69	2444551.957	16.29	2444552.028	15.69
2444552.863	15.99	2444552.926	15.80	2444552.984	15.82
2444609.758	16.47	2444609.759	16.46	2444609.849	15.78
2444609.890	16.35	2444609.894	16.16	2444609.968	15.66
2444609.970	15.70	2444610.015	16.41	2444636.710	16.09
2444636.818	15.75	2444636.956	15.75	0.000	16.27(±.02)
II V306					
2444636.697	17.42	2444636.807	17.89	2444636.945	17.95
2444912.879	17.48	2444912.944	17.72	2444912.995	17.83
2444960.727	17.70	2444960.821	17.84	2444960.892	17.66
2444961.726	17.77	2444961.813	17.68	2444961.878	17.79
2444961.966	16.58	2444962.027	17.06	2444962.876	17.64
2444962.948	16.59	2444963.021	17.12	2444994.647	17.80
2444994.753	17.85	2444994.843	17.77	2444994.937	16.53
2444995.620	17.68	2444995.749	17.83	2444995.812	17.79
2444995.909	16.42	2444995.965	16.83	0.000	17.88(±.03)
II V401					
2444908.886	17.28	2444908.953	17.17	2444909.001	17.44
2444960.734	18.04	2444960.825	18.20	2444960.937	18.16
2444961.730	18.01	2444961.817	18.17	2444961.882	18.25
2444961.969	18.24	2444962.053	16.79	2444962.880	18.21
2444962.953	18.22	2444963.054	16.84	2444994.652	18.22
2444994.758	18.21	2444994.848	17.14	2444994.942	17.64
2444995.624	18.39	2444995.744	18.34	2444995.821	16.89
2444995.915	17.57	0.000	18.02(±.05)		
II V407					
2444912.893	17.72	2444912.961	18.39	2444913.008	17.76
2444960.740	18.05	2444960.837	17.75	2444961.735	18.42
2444961.821	17.69	2444961.887	18.10	2444961.975	17.80
2444962.885	17.95	2444962.959	17.69	2444994.658	18.18
2444994.763	17.84	2444994.853	17.84	2444994.946	18.15
2444995.630	17.99	2444995.739	17.74	2444995.825	17.84
2444995.917	18.22	2445026.687	17.73	2445026.692	17.68
2445026.698	17.64	2445026.702	17.76	0.000	18.11(±.06)

HJD	B	HJD	B	HJD	B
II V501					
2444912.902	16.30	2444912.965	16.59	2444913.011	16.81
2444960.755	16.82	2444960.843	16.22	2444961.739	16.13
2444961.825	16.55	2444961.891	16.82	2444961.978	16.18
2444962.892	16.22	2444962.962	16.59	2444962.966	16.62
2444994.662	16.86	2444994.770	16.15	2444994.857	16.58
2444994.951	16.83	2444995.633	16.17	2444995.734	16.66
2444995.767	16.84	2444995.829	16.68	2444995.921	16.18
0.000	16.48(±.01)				
II V502					
2444960.753	19.20	2444960.851	18.18	2444961.833	17.92
2444961.896	18.38	2444961.983	19.01	2444962.033	19.07
2444962.897	18.34	2444962.976	18.80	2444963.032	19.07
2444994.670	18.82	2444961.746	19.23	2444994.955	19.15
2444995.638	18.70	2444995.727	19.04	2444995.777	19.18
2444995.831	19.10	2444995.925	19.18	2444995.971	19.11
2445026.707	18.07	2445026.721	17.77	2445026.750	18.01
2445026.788	18.28	2445026.794	18.44	2445026.830	18.61
2445026.880	18.83	2445027.658	19.21	2445027.692	19.05
2445028.639	19.15	2445028.782	18.20	2445028.835	18.57
2445322.770	19.05	2445349.717	18.07	2445349.738	17.89
2445349.750	18.06	0.000	18.23(±.04)		
II V504					
2444912.871	16.76	2444912.930	17.00	2444912.934	17.00
2444912.991	17.35	2444960.717	16.73	2444960.817	17.11
2444960.887	17.38	2444961.758	17.26	2444961.838	17.29
2444961.901	16.74	2444961.988	16.92	2444962.764	17.30
2444962.768	17.14	2444962.903	16.85	2444962.982	17.31
2444994.623	16.93	2444994.626	16.91	2444994.629	16.79
2444994.740	17.40	2444994.839	16.74	2444994.931	16.96
2444995.616	17.38	2444995.752	16.76	2444995.809	16.75
2444995.902	17.28	0.000	16.78(±.04)		
II V601					
2445322.797	17.95	2445322.801	18.03	2445322.866	17.98
2445322.953	18.13	2445322.996	18.10	2445323.064	17.79
2445323.772	17.58	2445323.863	17.82	2445323.906	18.05
2445323.966	18.13	2445324.030	18.09	2445324.771	17.38
2445324.953	17.95	2445324.997	17.98	2445325.032	18.08
2445327.898	18.01	2445354.897	18.15	2445355.769	17.75
2445355.811	17.82	2445355.774	17.76	2445355.870	17.97
2445355.899	18.02	2445355.984	18.15	0.000	18.51(±.03)

TABLE 4—*Continued*

HJD	B	HJD	B	HJD	B
III V101					
2445026.798	17.56	2445026.801	17.37	2445026.857	17.40
2445028.645	17.63	2445028.700	17.56	2445028.788	17.18
2445028.848	15.79	2445028.906	16.56	2445285.906	17.34
2445286.905	17.21	2445286.935	17.13	2445286.985	16.54
2445287.023	16.43	2445287.878	17.24	2445287.880	17.12
2445287.923	16.65	2445287.976	16.40	2445288.020	16.55
2445322.786	17.16	2445322.872	17.23	2445322.999	17.03
2445323.008	16.95	2445323.827	17.24	2445323.877	17.35
2445323.914	17.41	2445323.974	16.64	2445323.976	16.63
2445324.959	15.82	2445325.002	16.14	0.000	17.70(±.02)
III V102					
2445026.806	17.03	2445026.808	17.09	2445026.860	17.10
2445028.648	17.04	2445028.706	17.02	2445028.791	16.86
2445028.851	15.77	2445285.898	15.93	2445285.901	15.97
2445285.947	16.11	2445285.984	16.38	2445286.908	16.30
2445286.938	16.51	2445286.990	16.69	2445287.026	16.87
2445287.884	16.54	2445287.926	16.76	2445287.978	16.88
2445288.023	16.96	2445322.805	16.92	2445322.875	16.99
2445322.964	16.93	2445314.015	16.93	2445323.829	17.03
2445323.880	16.97	2445323.918	17.00	2445323.981	15.92
2445323.983	15.86	2445324.972	15.94	2445325.009	16.25
0.000	16.69(±.01)				
III V103					
2444960.766	19.40	2444960.858	18.75	2444961.768	19.11
2444961.844	18.06	2444961.931	18.78	2444961.993	19.16
2444962.040	19.32	2444962.986	19.29	2444962.909	18.90
2444963.039	19.33	2444994.680	19.12	2444994.784	19.31
2444994.878	19.30	2444994.970	18.15	2444995.648	19.35
2444995.718	19.22	2444995.792	19.23	2444995.843	19.01
2444995.933	18.31	2444995.985	18.72	2445026.732	18.50
2445026.737	18.41	2445026.742	18.44	2445026.812	19.08
2445026.864	19.11	2445026.899	19.10	2445027.667	18.51
2445027.711	18.83	2445028.653	18.82	2445028.714	19.04
2445287.892	18.35	2445287.933	18.47	2445287.983	18.66
2445287.892	18.55	2445287.933	18.56	2445287.983	18.75
2445322.746	19.37	2445322.880	18.46	2445323.021	18.90
2445323.850	18.49	2445323.856	18.54	2445323.886	18.73
2445323.922	18.91	2445323.988	19.15	2445355.992	18.53
2445356.011	18.76	0.000	18.61(±.02)		

HJD	B	HJD	B	HJD	B
III V201					
2444960.783	16.74	2444960.785	16.67	2444960.871	16.82
2444961.774	16.76	2444961.851	16.87	2444961.936	16.81
2444962.000	16.57	2444962.914	16.91	2444962.991	15.63
2444994.685	16.01	2444994.789	16.62	2444994.881	16.90
2444994.964	16.98	2444995.653	16.02	2444995.713	16.40
2444995.849	16.80	2444995.940	16.90	2445026.643	16.74
2445026.675	15.40	2445026.678	15.43	2445026.681	15.41
2445026.867	16.54	2445027.626	16.28	2445027.628	16.10
2445027.639	15.70	2445027.642	15.54	2445027.653	15.41
2445027.683	15.55	2445027.716	15.89	2445028.635	15.36
2445028.658	15.58	2445355.833	15.87	2445355.855	16.17
2445355.845	16.09	0.000	16.17(±.01)		
III V202					
2445026.819	16.46	2445026.821	16.49	2445026.870	16.64
2445028.660	16.75	2445028.720	17.01	2445028.758	16.90
2445028.800	16.95	2445028.863	16.89	2445028.866	16.86
2445285.925	17.10	2445285.951	16.95	2445285.956	16.88
2445285.988	16.34	2445285.999	16.12	2445286.912	16.91
2445286.941	16.93	2445286.993	16.94	2445287.028	16.93
2445287.897	16.46	2445287.937	16.60	2445287.987	16.71
2445288.026	16.80	2445322.888	16.15	2445322.890	16.15
2445322.914	15.99	2445322.916	16.02	2445322.919	16.04
2445322.972	16.35	2445323.026	16.58	2445323.931	17.02
2445323.993	16.97	0.000	17.33(±.02)		
III V203					
2444960.777	18.53	2444960.866	18.65	2444961.780	18.32
2444961.856	18.52	2444961.941	18.55	2444962.005	18.55
2444962.046	18.56	2444962.920	17.67	2444962.996	18.04
2444963.006	18.26	2444994.689	17.83	2444994.794	18.20
2444994.886	18.50	2444994.978	18.49	2444995.657	18.66
2444995.710	18.60	2444995.853	17.82	2444995.944	17.60
2444995.993	17.91	2445026.747	18.66	2445026.824	18.71
2445026.874	18.52	2445027.679	17.51	2445027.705	17.71
2445028.663	18.64	2445028.761	18.50	2445028.803	18.67
2445028.899	17.83	2445287.956	18.53	2445287.995	18.64
2445288.030	18.68	2445322.809	18.63	2445322.928	18.51
2445323.033	17.97	2445323.816	17.99	2445323.820	17.96
2445323.911	18.23	2445323.996	18.47	2445325.038	17.71
0.000	17.94(±.01)				

TABLE 4—*Continued*

HJD	B	HJD	B	HJD	B
III V204					
2444961.860	17.29	2444961.946	17.03	2444962.010	16.34
2444962.925	17.27	2444963.002	17.37	2444994.694	16.86
2444994.798	16.54	2444994.890	17.01	2444994.983	17.20
2444995.661	17.30	2444995.705	17.29	2444995.858	16.30
2444995.949	16.74	2445026.762	17.20	2445026.837	17.32
2445028.765	17.05	2445028.806	17.19	2445028.810	17.26
2445028.869	17.34	2445028.668	16.70	2445286.921	17.21
2445286.948	17.19	2445286.999	17.24	2445287.031	17.28
2445287.905	16.97	2445287.939	17.11	2445287.998	17.24
2445322.824	16.75	2445323.794	16.62	2445323.811	16.24
0.000	16.42(±.02)				
III V206					
2444961.797	16.49	2444961.863	16.90	2444961.949	17.44
2445692.013	17.61	2444962.928	17.07	2444963.006	17.50
2444994.698	17.91	2444994.801	16.79	2444994.892	17.39
2444994.994	17.82	2444994.701	17.76	2444995.664	17.79
2444995.702	17.83	2444995.865	16.94	2444995.952	17.39
2445026.765	17.08	2445026.840	17.47	2445028.671	17.84
2445028.768	16.50	2445028.812	16.80	2445028.873	17.23
2445285.916	17.83	2445285.920	17.70	2445285.961	17.80
2445286.010	17.74	2445286.944	17.71	2445286.914	17.68
2445287.003	17.83	2445287.037	17.64	2445287.901	17.41
2445287.949	17.61	2445288.003	17.73	2445322.827	16.65
2445322.912	17.21	2445322.978	17.42	2445323.039	17.70
2445323.799	17.78	2445323.891	16.78	2445323.935	17.01
2445324.000	17.40	0.000	16.60(±.01)		
III V208					
2444960.793	17.36	2444960.875	17.59	2444961.802	17.56
2444961.869	17.21	2444961.953	16.77	2444962.018	17.07
2444962.931	16.80	2444963.010	17.16	2444994.710	17.35
2444994.804	17.43	2444994.999	17.31	2444995.671	17.38
2444995.699	17.48	2444995.872	16.93	2444995.957	17.19
2444996.005	17.67	2445026.772	17.40	2445026.843	17.33
2445026.889	16.88	2445028.673	17.51	2445028.773	16.94
2445028.814	16.81	2445285.930	16.98	2445285.967	17.08
2445286.005	17.34	2445286.927	17.23	2445287.007	17.50
2445287.042	17.30	2445287.911	17.39	2445287.960	17.41
2445288.008	17.04	2445288.038	16.85	2445322.833	17.29
2445322.893	16.82	2445322.980	17.01	2445322.988	17.01
2445323.047	17.36	2445323.801	17.01	2445323.894	16.94
2445323.938	17.01	2445324.003	17.48	2445324.006	17.48

HJD	B	HJD	B	HJD	B
2445324.033	17.53	2445324.978	17.56	2445325.015	17.40
0.000	18.61(±.02)				
III V302					
2444961.720	17.15	2444961.807	17.40	2444961.873	17.46
2444961.957	17.41	2444962.022	17.63	2444962.936	17.34
2444963.015	17.46	2444994.714	17.31	2444994.808	17.45
2444994.903	17.48	2444995.005	17.45	2444995.680	16.68
2444995.694	16.75	2444995.878	17.35	2444995.962	17.51
2445026.778	17.53	2445026.846	17.40	2445028.680	16.88
2445028.775	17.29	2445028.820	17.37	2445028.889	17.48
2445285.936	17.51	2445285.978	17.55	2445286.016	16.76
2445286.955	17.46	2445286.975	17.47	2445287.014	17.53
2445287.047	17.54	2445287.916	17.20	2445287.966	17.29
2445288.013	17.46	2445322.858	17.31	2445322.907	16.31
2445322.910	16.35	2445322.992	16.84	2445324.010	16.62
0.000	18.24(±.02)				
IV V103					
2444856.681	16.72	2444856.684	16.67	2444856.758	16.79
2444856.833	16.63	2444856.887	16.59	2444856.944	16.70
2444856.989	16.26	2444857.726	16.15	2444857.760	16.25
2444857.840	16.50	2444857.899	16.54	2444857.956	16.61
2444858.007	16.75	2444858.897	15.93	2444853.945	15.97
2444858.995	16.09	2444883.689	16.81	2444883.741	16.72
2444883.849	16.73	2444883.959	16.15	2444883.964	15.96
2444884.660	16.14	2444912.630	16.60	2444912.697	16.38
2444912.765	15.84	2444912.795	15.97	2444912.813	16.02
2444912.857	16.23	2444914.631	16.09	2444914.672	16.28
2444914.703	16.35	2444960.670	16.31	2444960.680	16.41
2444960.696	16.47	2444961.618	16.58	2444961.628	16.65
2444961.639	16.73	2444961.655	16.73	2444961.702	16.08
2444961.710	16.01	2445322.638	16.68	2445323.599	15.96
2445323.602	16.01	2445323.604	16.01	2445323.606	16.03
0.000	17.90(±.02)				
IV V104					
2444856.692	17.46	2444856.760	18.01	2444856.891	18.32
2444856.948	18.42	2444857.695	17.25	2444857.903	18.40
2444857.960	18.47	2444883.750	18.27	2444883.746	18.16
2444884.693	17.84	2445285.639	17.36	2445285.642	17.36
2445285.732	17.68	2445285.799	18.05	2445285.841	18.14
2445286.633	18.10	2445286.686	17.36	2445286.753	17.74
2445287.708	17.44	2445287.756	17.53	2445287.801	17.74
2445287.825	17.76	2445288.614	18.47	2445349.641	18.33

TABLE 4—*Continued*

HJD	B	HJD	B	HJD	B
0.000	17.35(±.02)				
IV V105					
2444856.953	18.63	2444857.001	17.80	2444857.909	18.55
2444857.967	18.53	2444883.757	18.47	2444883.861	18.53
2444883.960	18.64	2444884.687	17.78	2445285.652	18.42
2445285.740	17.34	2445285.808	17.62	2445286.641	18.39
2445286.693	18.51	2445287.713	18.49	2445287.762	18.33
2445322.629	18.15	2445322.634	18.13	2445323.590	17.69
2445323.595	17.54	2445323.652	17.91	2445324.601	17.66
2445324.637	17.48	2445324.672	17.73	2445324.708	17.88
0.000	15.96(±.02)				
IV V106					
2444856.710	17.55	2444856.772	16.27	2444856.848	16.67
2444856.901	17.18	2444856.958	17.41	2444856.992	17.50
2444857.699	17.14	2444857.781	16.64	2444857.783	16.69
2444857.858	16.85	2444857.915	17.32	2444857.970	17.52
2444858.010	17.78	2444858.865	17.46	2444858.912	17.45
2444858.961	17.60	2444858.992	17.68	2444883.696	16.86
2444883.700	16.81	2444883.776	17.26	2444883.864	17.68
2444883.947	17.80	2444884.663	16.77	2444884.723	17.33
2444884.727	17.32	2444912.636	17.74	2444912.639	17.57
2444912.702	17.49	2444912.705	17.45	2444912.772	17.68
2444912.802	17.54	2444912.823	16.72	2444912.827	16.56
2444912.830	16.43	2444912.834	16.30	2444912.838	16.21
2444912.841	16.28	2444912.843	16.30	2444914.646	17.70
2444914.679	17.31	2444914.686	17.39	2444914.711	17.55
2444914.718	17.63	2444958.641	17.72	2444958.658	17.73
2445322.645	16.75	2445322.648	16.80	2445323.609	16.81
2445323.612	16.77	0.000	17.31(±.03)		
IV V107					
2444856.714	18.08	2444856.780	18.09	2444856.851	18.07
2444856.905	18.08	2444856.962	18.14	2444857.917	18.14
2444857.974	17.86	2444858.970	17.94	2444858.988	18.02
2444883.780	18.04	2444883.784	18.11	2444883.869	18.13
2444883.952	17.92	2444884.671	17.62	2445285.658	17.97
2445285.744	18.16	2445285.813	17.42	2445286.654	17.96
2445286.697	18.14	2445286.759	18.09	2445287.720	17.90
2445287.767	17.95	2445287.806	18.09	2445322.619	17.47
2445322.622	17.47	2445323.659	17.37	2445323.661	17.36
2445323.664	17.21	2445323.667	17.26	2445323.684	17.28
2445323.690	17.35	2445323.703	17.27	2445323.705	17.26
0.000	18.21(±.03)				

HJD	B	HJD	B	HJD	B
IV V108					
2444856.716	16.96	2444856.719	16.82	2444856.783	17.00
2444856.855	16.54	2444856.909	16.52	2444856.966	16.81
2444857.794	16.83	2444857.865	17.13	2444857.921	16.94
2444857.978	16.49	2444858.871	16.81	2444858.919	16.91
2444858.974	17.09	2444883.703	16.77	2444883.706	16.89
2444883.789	17.05	2444883.791	17.11	2444883.873	16.48
2444884.668	16.53	2444912.644	17.06	2444912.646	17.15
2444912.649	17.11	2444912.653	17.15	2444912.656	17.17
2444912.659	17.14	2444912.662	17.12	2444912.664	17.13
2444912.668	17.11	2444912.671	17.08	2444912.673	17.14
2444912.676	17.11	2444912.678	17.01	2444912.689	17.00
2444912.717	16.69	2444912.720	16.66	2444912.722	16.60
2444912.726	16.56	2444912.732	16.56	2444912.737	16.50
2444912.742	16.49	2444912.748	16.51	2444912.754	16.53
2444912.757	16.46	2444912.806	16.69	2444912.853	16.87
2444914.650	16.50	2444914.653	16.52	2444914.698	16.49
0.000	16.26(±.01)				
IV V122					
2444856.793	15.53	2444856.869	15.36	2444856.923	15.37
2444856.976	16.10	2444856.979	16.07	2444857.884	15.34
2444857.932	15.68	2444857.997	15.29	2444858.017	15.31
2444858.835	15.43	2444858.880	15.35	2444858.930	16.10
2444858.984	15.35	2444883.679	15.42	2444883.682	15.42
2444883.684	15.32	2444883.708	15.36	2444883.813	15.43
2444883.916	15.74	2444883.920	15.74	2444884.651	15.40
2444912.709	15.34	2444912.712	15.38	2444912.714	15.34
2444912.778	16.04	2444912.791	15.95	2444912.810	15.57
2444912.866	15.43	2444914.616	15.53	2444914.618	15.55
2444914.655	15.40	2444914.661	15.38	2444914.665	15.35
2444914.666	15.36	2444914.668	15.39	2444914.700	15.46
2444914.721	15.87	2444914.725	16.01	2444914.727	15.95
2444914.730	16.05	2444914.732	15.98	2444914.734	16.04
2444914.736	16.01	2444962.626	15.38	2444962.634	15.37
2444962.637	15.36	2444962.641	15.34	2444962.644	15.29
2444962.651	15.29	2444958.616	15.33	2444958.627	15.37
0.000	16.74(±.03)				
IV V201					
2445285.623	17.40	2445285.627	17.42	2445285.719	17.52
2445285.722	17.32	2445285.779	16.69	2445285.826	16.13
2445286.614	17.39	2445286.617	17.31	2445286.679	17.03
2445286.738	16.29	2445286.744	16.20	2445286.783	16.56

TABLE 4—*Continued*

HJD	B	HJD	B	HJD	B
2445287.702	16.52	2445287.742	16.89	2445287.793	17.12
2445287.815	17.19	2445288.603	16.36	2445288.606	16.42
2445288.649	16.78	2445322.607	17.29	2445322.613	17.22
2445322.732	17.42	2445323.656	17.41	2445324.626	17.51
2445324.639	17.50	2445324.672	16.91	2445324.678	16.58
2445324.713	16.03	2445324.717	15.97	0.000	16.77(±.02)
IV V301					
2445285.665	16.52	2445285.748	16.73	2445285.822	16.95
2445285.817	16.88	2445286.658	17.10	2445286.706	17.00
2445286.774	16.26	2445286.777	16.33	2445286.780	16.29
2445287.724	16.87	2445287.771	16.89	2445287.812	16.96
2445287.835	17.00	2445288.642	16.25	2445322.654	16.59
2445322.657	16.55	2445322.651	16.62	2445322.717	16.16
2445322.721	16.17	2445323.616	16.78	2445313.620	16.82
2445324.622	16.28	2445324.646	16.42	2445324.711	16.57
2445324.713	16.58	2445349.613	16.72	0.000	17.85(±.03)
IV V401					
2445285.631	16.89	2445285.636	16.92	2445285.727	17.08
2445285.788	16.42	2445285.792	16.19	2445285.795	16.01
2445285.830	15.55	2445286.621	16.86	2445286.625	16.92
2445286.683	16.89	2445286.749	16.25	2445286.792	15.56
2445286.704	17.15	2445287.704	17.15	2445287.747	15.39
2445287.749	15.42	2445287.751	15.45	2445287.797	15.91
2445287.820	16.15	2445288.609	16.96	2445288.691	15.42
2445322.663	16.82	2445322.670	16.87	2445322.725	16.70
2445323.622	16.81	2445323.624	16.91	2445323.696	16.44
2445323.711	15.83	2445323.714	15.79	2445323.716	15.69
2445324.608	16.99	2445324.640	16.80	2445324.690	15.71
2445324.699	15.71	2445349.603	16.82	2445349.646	15.54
2445349.650	15.56	2445349.658	15.67	0.000	17.82(±.02)

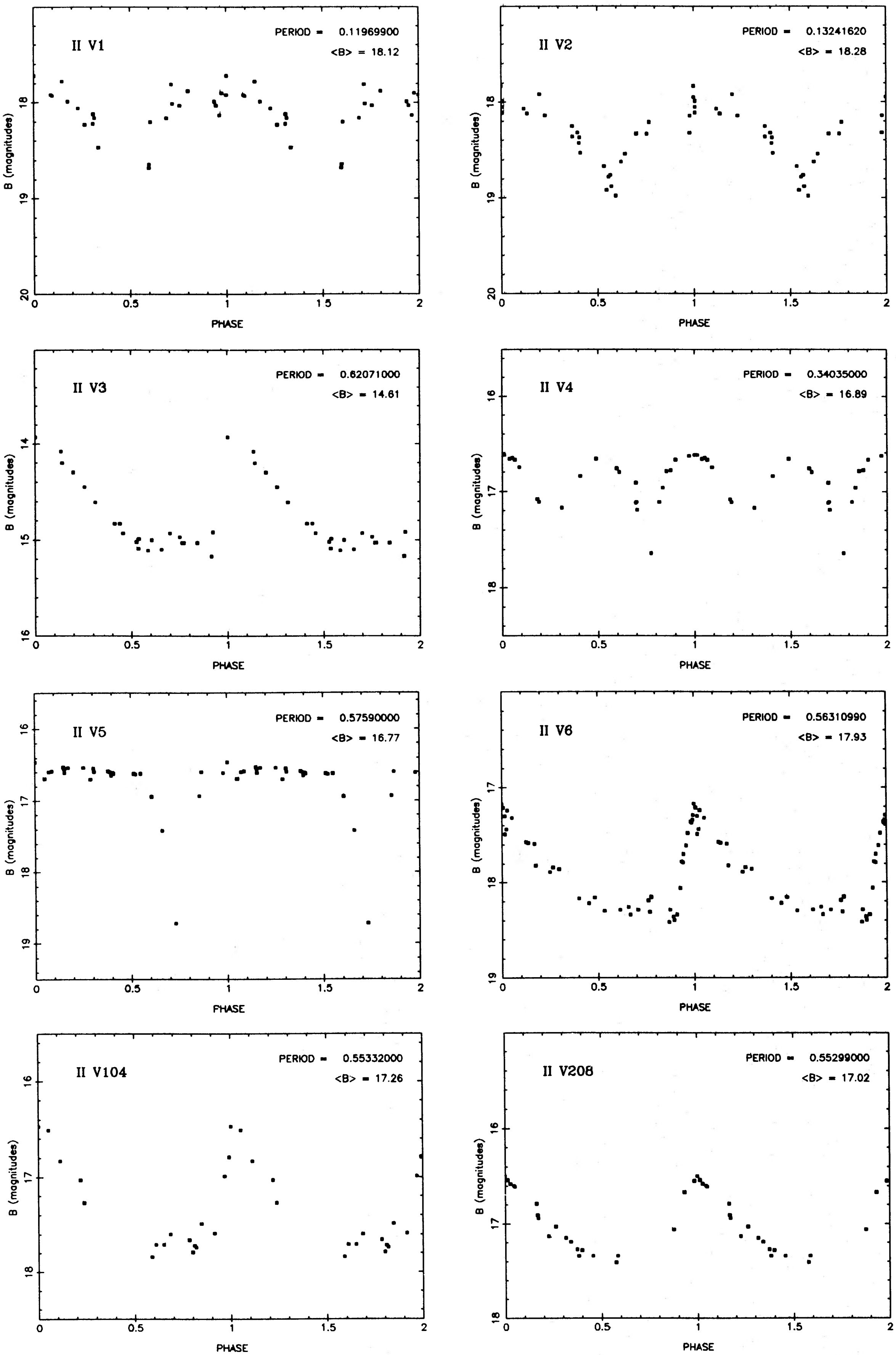

FIG. 4.—The light curves in *B* obtained with SIT Vidicon photometry are presented. Periods and mean magnitudes are quoted for each object. Two cycles are shown for the sake of clarity, so that each data point is plotted twice.

1984ApJ...283..580S

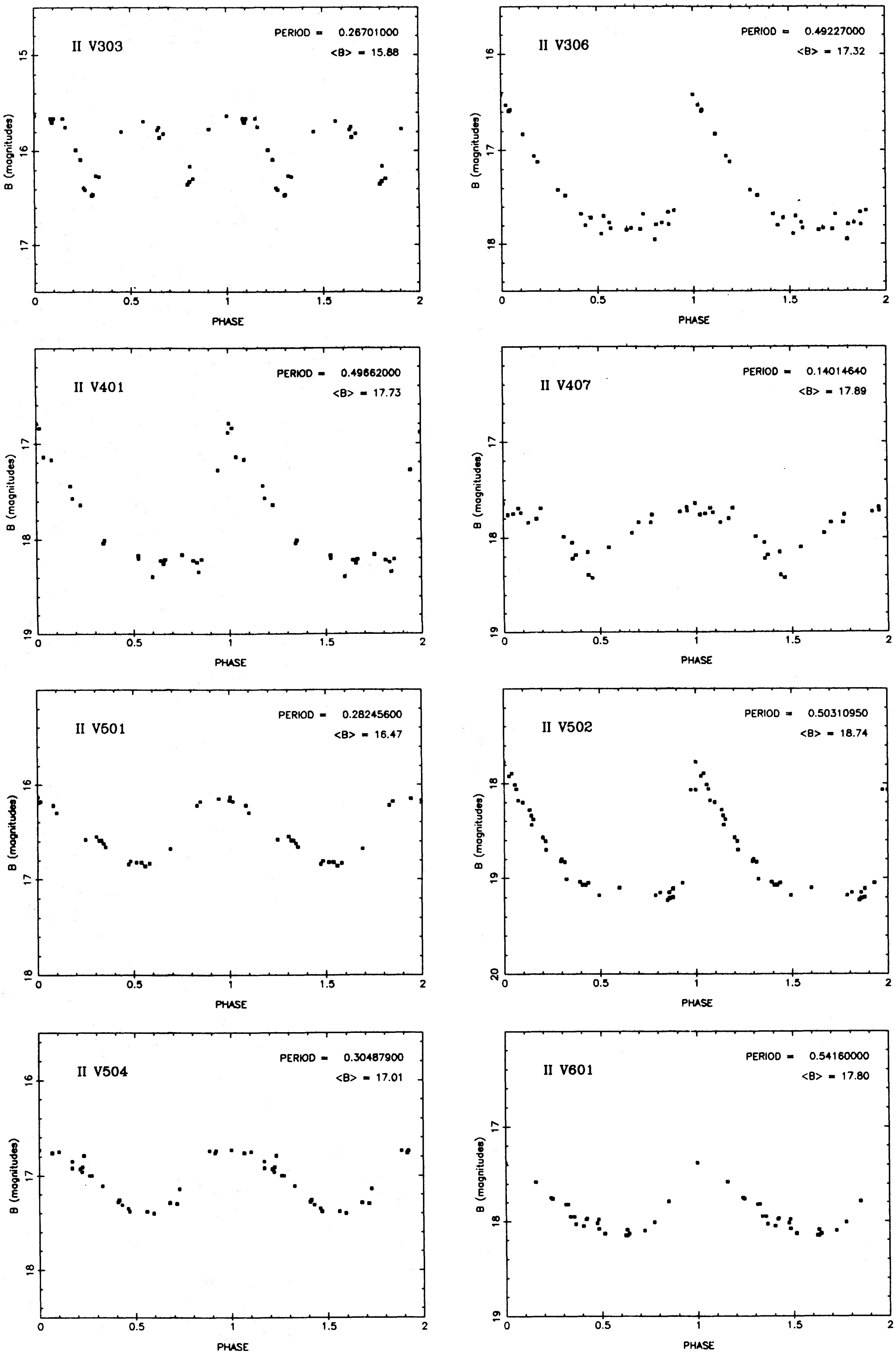

FIG. 4.—*Continued*

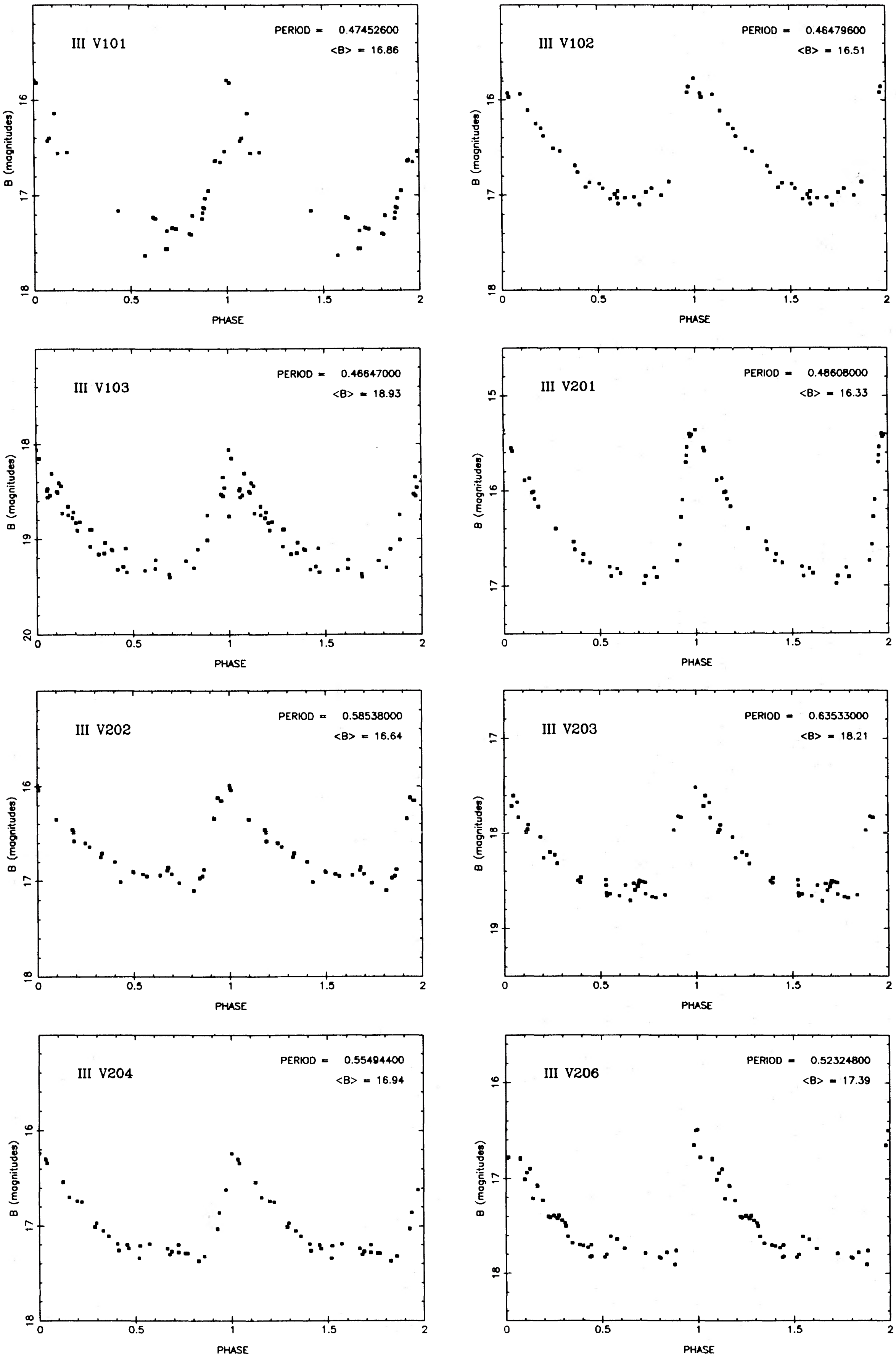

FIG. 4.—*Continued*

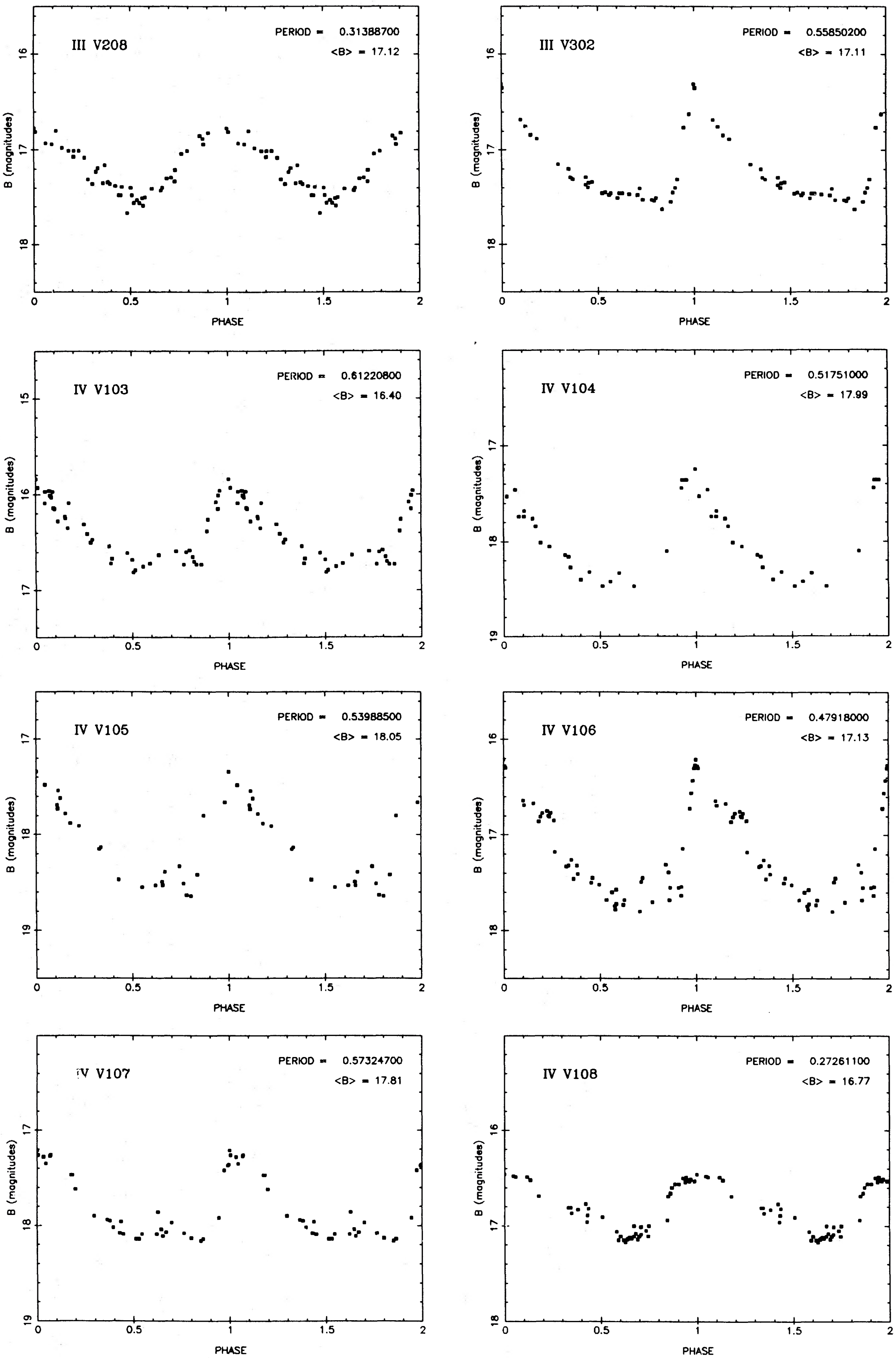

FIG. 4.—*Continued*

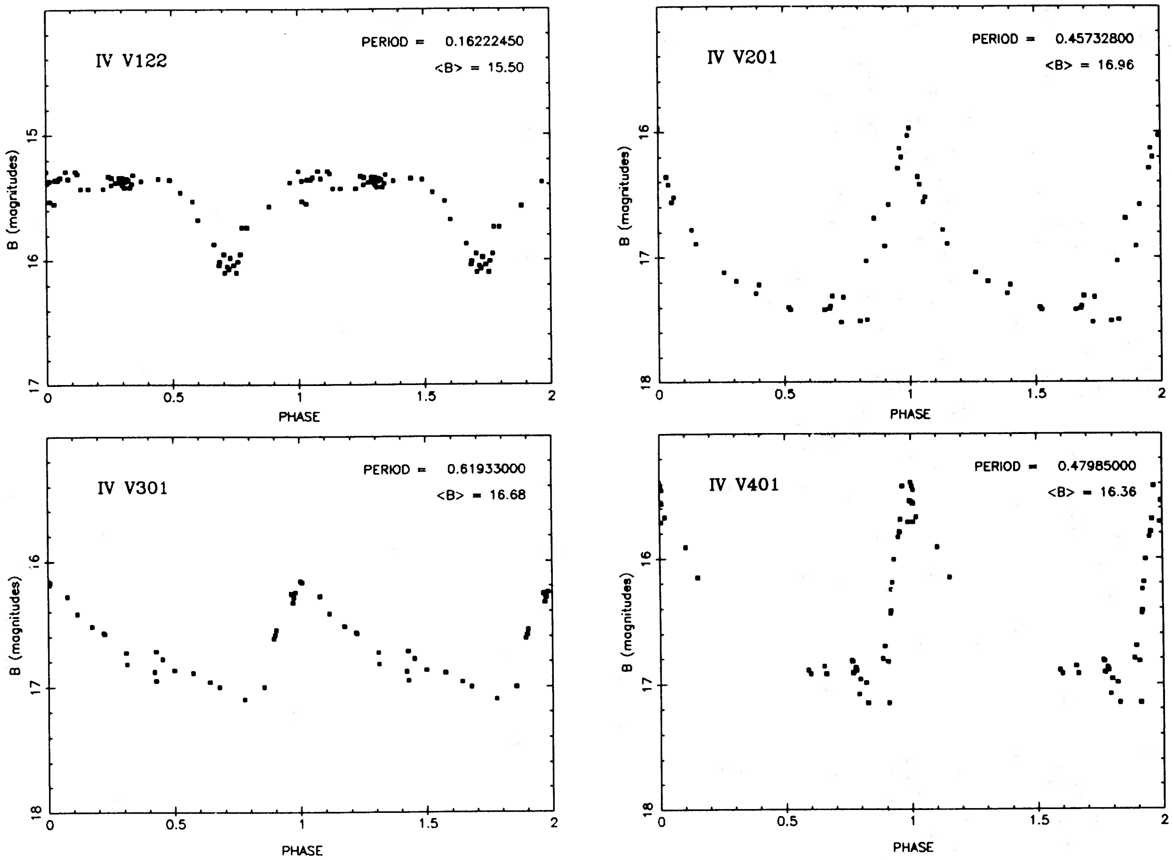

FIG. 4.—*Continued*

TABLE 5

EPHEMERIDES

Object	P(days)	ΔP(days)	Θ	$\langle B \rangle$	Epoch(HJD)	Type
II V1	0.119699	0.0000033	0.58	18.12	2,444,609.974	E
II V2	0.1324162	0.000032	0.24	18.28	2,444,636.732	E
II V3	0.620710	0.000059	0.47	14.61	2,444,636.973	RR*ab*
II V4	0.340350	0.000009	0.67	16.89	2,444,609.774	E
II V5	0.5759	0.0008	1.11	16.77	2,444,551.945	E
II V6	0.5631099	0.0000014	0.11	17.93	2,445,355.971	RR*ab*
II V104	0.553320	0.0000026	0.26	17.26	2,445,324.991	RR*ab*
II V208	0.55299	0.00007	0.19	17.02	2,445,349.688	RR*ab*
II V303	0.267010	0.000006	0.47	15.88	2,444,609.758	E
II V306	0.49227	0.00014	0.33	17.32	2,444,995.909	RR*ab*
II V401	0.49662	0.00008	0.24	17.73	2,444,994.848	RR*ab*
II V407	0.140146	0.0000023	0.32	17.89	2,444,961.736	?
II V501	0.282456	0.000053	0.24	16.47	2,444,961.740	RR*c*
II V502	0.5031095	0.000001	0.17	18.74	2,445,026.722	RR*ab*
II V504	0.304879	0.00002	0.24	17.01	2,444,960.717	RR*c*
II V601	0.54160	0.000015	0.42	17.80	2,445,324.771	RR*ab*
III V101	0.474526	0.000005	0.27	16.86	2,445,028.848	RR*ab*
III V102	0.464796	0.000052	0.19	16.51	2,445,028.851	RR*ab*
III V103	0.46647	0.00003	0.27	18.93	2,444,961.845	RR*ab*
III V201	0.486080	0.000015	0.07	16.33	2,445,028.635	RR*ab*
III V202	0.58538	0.000018	0.17	16.64	2,445,322.914	RR*ab*
III V203	0.63533	0.00004	0.17	18.21	2,445,027.679	RR*ab*
III V204	0.554944	0.00005	0.16	16.94	2,445,323,812	RR*ab*
III V206	0.523248	0.000005	0.26	17.39	2,444,961.797	RR*ab*
III V208	0.313887	0.000004	0.20	17.12	2,444,961.953	RR*c*
III V302	0.558502	0.000022	0.17	17.11	2,445,322.907	RR*ab*
IV V103	0.612208	0.000020	0.14	16.40	2,444,912.765	RR*ab*
IV V104	0.517510	0.000021	0.23	17.99	2,444,857.695	RR*ab*
IV V105	0.539885	0.00004	0.23	18.05	2,445,285.741	RR*ab*
IV V106	0.47918	0.00005	0.12	17.13	2,444,912.838	RR*ab*
IV V107[a]	0.573247	0.00002	0.11	17.81	2,445,323.665	RR*ab*
IV V108	0.272611	0.00001	0.09	16.77	2,444,912.758	RR*c*
IV V122	0.1622245	0.000008	0.11	15.50	2,444,856.979	E
IV V201	0.457328	0.000016	0.15	16.96	2,445,324.713	RR*ab*
IV V301[a]	0.619330	0.000030	0.203	16.68	2,445,322.717	RR*ab*
IV V401	0.479850	0.000084	0.14	16.36	2,445,287.750	RR*ab*

[a] Period determined from plate material.

object was inferred to be. For eclipsing stars (E), phase is taken to be zero at minimum light, whereas for the RR Lyrae stars (R), phase zero is at maximum light, according to convention.

The light curves obtained from the photometry with the SIT camera are presented in Figure 4. For the RR Lyrae stars, the phase at maximum light has been set to zero. No attempt has been made to set the phase zero point for the eclipsing stars. In addition to furnishing reliable periods so that follow up spectroscopy can be done at the appropriate phase, the light curves in B make it possible to investigate these stars along the lines of Sandage, Katem, and Sandage (1981) and Sandage (1981*a*, *b*, 1982*a*, *b*), who have studied the absolute magnitudes and chemical compositions of RR Lyrae stars on the basis of the light curve morphology alone.

VII. THE ECLIPSING VARIABLES

It is worth a digression at this point to draw attention to the eclipsing variables that have been found. A few of these have been studied photoelectrically, and the results have been stated in Tables 3–5, although it has not been possible to look at the majority of them in any detail (there are twice as many of them per field as RR Lyrae stars). The light curves and periods of the ones that have been studied here indicate that a large fraction of these are W UMa type contact binaries. Some of them are as faint as 18.5 mag and so are apparently several kpc from the disk and are probably halo objects. Mochnacki (1981*a*, *b*) has shown that absolute magnitudes of W UMa type stars can be derived to an accuracy of 0.3 mag without requiring a complete radial velocity curve. Spectroscopic observations at a few strategic phases allow the center of mass velocity to be determined. These are therefore potential probes of the galactic halo.

VIII. CONCLUDING REMARKS

The space density distribution of the RR Lyrae stars found in this survey, as well as their chemical composition and kinematics, will be discussed after the results of spectroscopy and spectrophotometry are presented in another paper.

The author thanks Dr. J. B. Oke for many invaluable discussions and is grateful to Palomar Observatory for financial support during the course of this project.

REFERENCES

Butler, D., Kemper, E., Kraft, R. P., and Suntzeff, N. B. 1982, *A.J.*, **87**, 353.
Kinman, T. D. 1972, *Quart. J.R.A.S.*, **13**, 258.
Kinman, T. D., Mahaffey, C. T., and Wirtanen, C. A. 1982, *A.J.*, **87**, 314.
Lafler, J., and Kinman, T. D. 1965, *Ap. J. Suppl.*, **11**, 216.
Mochnacki, S. W. 1981*a*, *Ap. J.*, **245**, 650.
———. 1981*b*, private communication.
Saha, A. 1983, Ph.D. thesis, California Institute of Technology.
Sandage, A. 1970, *Ap. J.*, **162**, 841.
Sandage, A. 1981*a*, *Ap. J.* (*Letters*), **244**, L23.
———. 1981*b*, *Ap. J.*, **248**, 161.
———. 1982*a*, *Ap. J.*, **252**, 553.
———. 1982*b*, *Ap. J.*, **252**, 574.
Sandage, A., Katem, B., and Sandage, M. 1981, *Ap. J. Suppl.*, **46**, 41.
Sandage, A., and Smith, L. W. 1963, *Ap. J.*, **137**, 1057.
Thuan, T. X., and Gunn, J. E. 1976, *Pub. A.S.P.*, **88**, 543.
Woolley, R. 1978, *M.N.R.A.S.*, **184**, 311.

A. SAHA: Kitt Peak National Observatory, P.O. Box 26732, Tucson, AZ 85726-6732.